

***Ab initio* studies on the stability and electronic structure of LiCoO₂ (003) surfaces**Liyun Hu,^{1,2} Zhihua Xiong,^{1,2,3} Chuying Ouyang,^{1,2} Siqi Shi,¹ Yinghua Ji,^{1,2,*} Minsheng Lei,² Zhaoxiang Wang,¹ Hong Li,¹ Xuejie Huang,¹ and Liqian Chen^{1,†}¹Laboratory for Solid State Ionics, Institute of Physics, Chinese Academy of Sciences, P.O. Box 603, Beijing 100080, China²Department of Physics, Jiangxi Normal University, Nanchang 330027, China³Department of Applied Physics, Jiangxi Science & Technology Normal University, Nanchang 330013, China

(Received 6 July 2004; published 31 March 2005)

The electronic structures of 2×2 polar (003) surfaces of LiCoO₂ have been studied using the first-principles projector augmented-wave (PAW) method within the generalized gradient approximation (GGA), based on the density functional theory (DFT). Several geometry structure models were considered with different terminations in order to obtain the most stable structure. From cleavage energies of separation it reveals that, for LiCoO₂ (003), the configuration with O termination on one side and Li termination on the other side was the most stable one. Because the exposed Li-O groups easily react with the electrolytes so that the structure is destroyed, this conclusion can indirectly explain the phenomenon that LiCoO₂ coated by MgO possesses the more stable structure [J. Electrochem. Soc. **149**, A466 (2002)]. It is also found that structure relaxation is considerably large, and the electronic density of states (DOS) shows large difference between (003) surfaces and bulk, with, for example, a decrease of the band gap between the valance band and the empty band in (003) surfaces region compared to the bulk. It is possible to reconstruct for the polar (003) surfaces of LiCoO₂ crystallite.

DOI: 10.1103/PhysRevB.71.125433

PACS number(s): 61.43.Bn, 71.15.Nc, 82.45.Jn, 82.47.Aa

I. INTRODUCTION

Considerable interest exists in the lithium-metal-oxides due to their application in rechargeable battery electrodes¹ and electrochemical properties.² Among them, layered LiCoO₂ has favorable attributes including high open circuit voltage, high capacity and energy density, and excellent cycle life. The LiCoO₂ crystal has an ordered rock structure such that lithium and cobalt occupy alternate (111) layers (Fig. 1). While, as one of the most widely studied of all cathode materials for the lithium ion battery, many studies of the electrochemical performance have been done, some questions still exit. To the best of our knowledge, no information about the geometric and electronic structure of polar surfaces is presently available, either from experiment or from theory. From a physical/chemical point of view, it is necessary and challenging to obtain the microscopic understanding of structure and stability of polar surfaces in surface science.³

It is well recognized that most clean polar surfaces are usually unstable and thus difficult to prepare unreconstructed and defect-free surfaces. They are so called “Tasker-3” surfaces.⁴ A number of mechanisms have been suggested for the stabilization of such polar surfaces. These include reconstruction of the surface, faceting, the presence of adsorbates, and changes in the surface electronic structure. These mechanisms were recently reviewed by Noguera.^{5,6} Although there are many reconstruction mechanisms for polar surfaces, in the present study we will first focus on the clean, unreconstructed (003) surfaces of LiCoO₂ to analyze their atomic and electronic properties.

Lacking experimental data on surfaces, we first focus on all possible (2×2) terminations and then give a possible reconstructed model. This provides a first database against which future models of reconstructed surfaces may be com-

pared, in particular by how much they would have to reduce the surface free energy of separation in order to have corresponding facets contribute significantly to the real LiCoO₂ crystal shape. In addition, relatively low surface free energies from (2×2) terminations might point at likely candidates for surface reconstructions. Through the study of material surface, we can get further comprehension for surface properties of material and obtain some information of relationship between surface characteristics and surface modifications. Thus, this will help us to improve material performance.

In the present work, we investigate two kinds of main crystal terminations of LiCoO₂ (003) surfaces. The fully relaxed geometric structures and cleavage energies were calculated using a first-principles density functional theory (DFT) method within the generalized gradient approximation

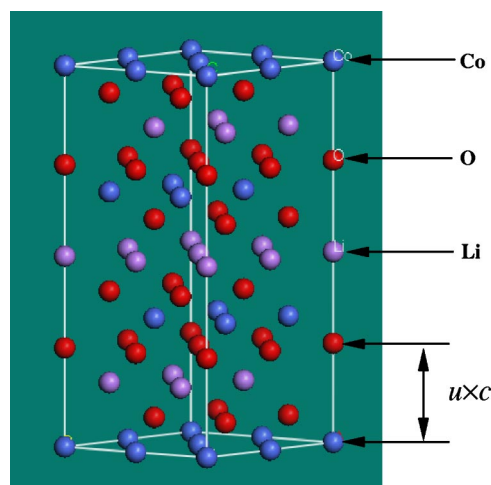


FIG. 1. (Color online.) Crystal structure of the layered LiCoO₂ with $R\bar{3}m$ symmetry.

TABLE I. Computed and experimental values of the structural parameters for bulk LiCoO_2 . a and c are the lattice constants. V is the volume of one formula of LiCoO_2 . Experimental values are from Ref. 22. Relative deviation from experiment is given in parentheses.

	GGA(this study)	Ref. 15	Ref. 16	Ref. 17	Expt.
$a(\text{\AA})$	2.84(+0.9%)	2.88	2.82	2.93	2.82
$c(\text{\AA})$	14.18(+0.7%)	14.04	14.04	13.20	14.08
c/a	4.99	4.88	4.51	4.99	
$V(\text{\AA}^3)$	33.07	32.20	32.23	32.71	
u	0.260	0.264	0.264	0.260	

(GGA). We will discuss geometric and electronic structure, and what is more, the relative stability of surfaces will be included. We will first briefly describe the method and the surface models used for the electronic structure calculations in Sec. II, and then in Sec. III we present the results on the clean and unreconstructed LiCoO_2 (003) surface, which include the electronic and geometric structure of surfaces. Finally, the relative stability of surfaces is discussed in Sec. IV. The conclusion will be summarized in Sec. V.

II. METHODS AND SURFACE MODELS

A. Methods

In this paper, we study the surfaces of LiCoO_2 (003) using the electron projector augmented wave (PAW) method,⁷ which was proposed by Blöchl⁷ for resolving the Kohn-Sham equations within the density-functional theory.⁸ The exchange and correlation energy was treated via the generalized gradient approximation⁹ using the Perdew-Wang (PW91) parametrization.¹⁰ Wave functions were expanded with a plane-wave (PW) basis set and energies cutoff of 550 and 800 eV were employed for bulk and surface calculations, respectively. The PAW formalism has numerical advantages for pseudopotential techniques. This relatively new technique has proven very accurate in comparison with other *ab initio* methods^{7,11,12} within the DFT framework. In the calculations, the core radii for the oxygen, lithium, and cobalt pseudopotentials were 1.06, 0.80, and 1.16 \AA , respectively. The O $2s$ and $2p$, Li $2s$, and Co $3d$ and $4s$ electrons were treated as valence electrons, and all the others were treated as core electrons. The Vienna *ab initio* simulation package^{13,14} (VASP) were used throughout this study.

To simulate surfaces we have used periodically reproduced slab supercells, possessing the same periodicity of spacing as the bulk in x and y directions and separated in z direction by a vacuum layer, which is considered to be thick enough to minimize the surface-surface interaction. All surfaces were represented by periodically repeated slabs consisting of 12 atomic layers and separated by a vacuum region of about 13–13.4 \AA , which was found to be sufficient for all surfaces considered. To stimulate underlying of bulk structure, the slab lattice constant in the direction parallel to the surface was always set equal to the theoretical equilibrium bulk value (see Table I). Here, slabs with 12 atomic layers

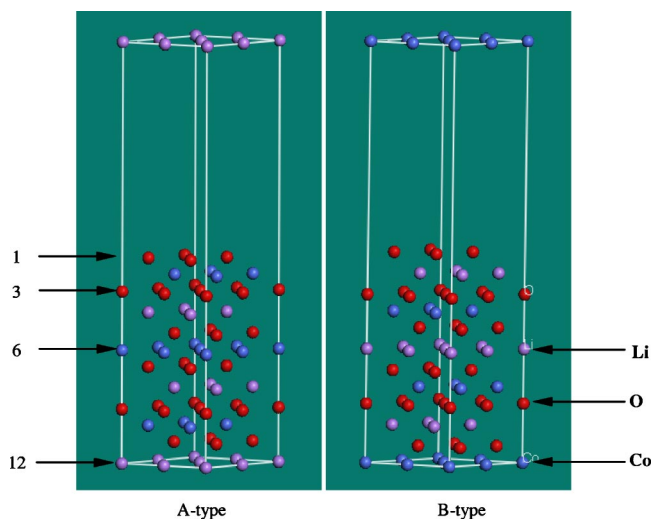


FIG. 2. (Color online.) Two clean and unreconstructed slab models with 12 atom layers obtained by cleaving the crystal perpendicular to the c axis. A type with O- and Li-terminated polar surface and B type with O- and Co-terminated polar surfaces.

(48 atoms) were used and the Brillouin zone of the supercell was sampled with a $(5 \times 5 \times 1)$ Monkhorst-Pack¹⁸ k -point grid. We also tested with $(6 \times 6 \times 1)$ mesh and no obvious differences were found. For the calculations on the polar surfaces we chose a plane wave cutoff energy 800 eV, which was sufficient to get well-converged results (within 1 meV per atom). Furthermore, a Gaussian broadening¹⁹ with a smearing parameter of 0.04 eV (0.2 eV for bulk) was included. However, the results for the 12-layer (003) slabs used in the present calculations have not been tested with respect to slab thickness convergence.

B. Surface models

It can be seen obviously that cleaving the LiCoO_2 crystal perpendicular to the c axis (see Fig. 1) always produces a crystal, which has a monolayer of cations on the surface and a monolayer of anions on the other in order to preserve charge neutrality and stoichiometry. In this sense, it may create simultaneously several possible models. If we only consider cuts containing 12 atomic layers parallel to the c axis, all slabs representing polar surfaces are automatically stoichiometric and are inevitably Li/Co termination on one side and O termination on the other side. In this study, we denote the slab model with O and Li terminations as A type and the slab model with O and Co terminations as B type. Plots of the clean, unrelaxed and unreconstructed slab configurations used in our work are shown in Fig. 2. From the top oxygen atomic layer to the bottom lithium/cobalt atomic layer, we indicated these layers by using 1–12 integers (see Fig. 2). Comparing to the structure of the bulk, A type and B type were obtained by breaking the Li-O and Co-O bonding interaction, respectively. Lattice constants c of slab supercell model for A type and B type were set equal to about 26.18 \AA , so the values of vacuum were corresponding to about 13.4 and 13 \AA due to the difference between the value of Li-O interlayer spacing and that of Co-O, respectively.

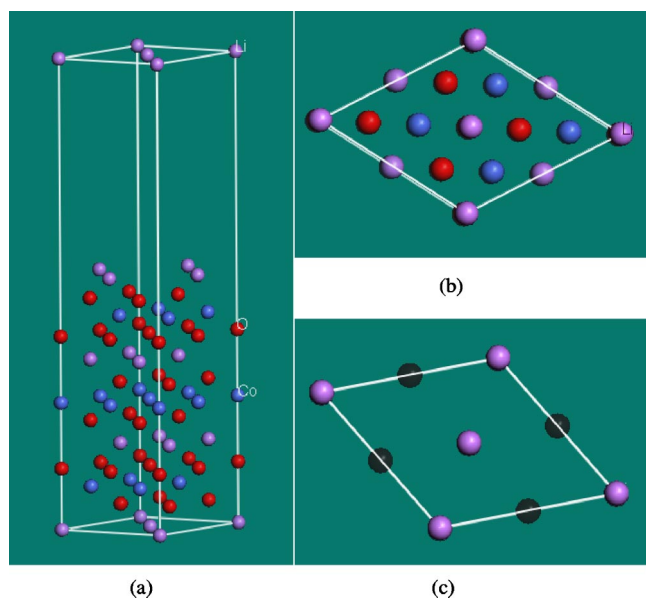


FIG. 3. (Color online.) Lithium terminations model used in the calculations of the (003) LiCoO₂ nonpolar surface. Lithium atoms are removed in a checkerboard style on both surfaces. (b) and (c) are view from the top of the surface. Only surface Li atoms are appeared in (c) and the bottom layer Li atoms are in gray.

For both types defined above, full relaxation for all slab atoms was performed to optimize the equilibrium positions by calculating the forces on atoms (smaller than 0.05 eV/Å), whereas the lattice constant *c* was kept fixed to 26.18 Å. The initial atomic positions in the surface slabs were chosen equal to our calculated equilibrium bulk value. The whole equilibrium atom-layer thicknesses calculated with GGA are 13.71 and 13.99 Å for *A* type and *B* type, respectively; both are smaller than those of bulk. For the clean, unreconstructed (003) surfaces the geometric relaxations of the surface were calculated using slabs containing 12 atomic layers.

In Sec. IV, the (003) surface was modeled as lithium-terminated surfaces with half of the surface lithium atoms moved from one side of the slab to the other in only one way to fulfill the LiCoO₂ formula. The configuration of lithium terminations considered here is schematically shown in Fig. 3, in which lithium atoms were removed in a checkerboard style on both surfaces. No symmetry was imposed on the system. The (003) surface has been calculated using slab with thickness of 13 layers. The initial interatomic distances in the surface slabs were set equal to our calculated equilibrium bulk values. For simplicity, the slab atoms were only allowed to fully relax in the *z* direction. Thus, the Hellmann-Feynmann forces were systematically calculated and the nuclei steadily relaxed towards the equilibrium positions until the forces became smaller than 0.05 eV/Å. The thickness of whole equilibrium atom layers is 0.80 Å smaller than that of bulk. According to previous discussion, it is necessary to point out that the introduction of surface leads to the decrease of all atom-layer thicknesses for all models mentioned above.

The relative stabilities of different surfaces were discussed in terms of their cleavage energies. The cleavage energy E_{cleav} is defined as the energy required for cleaving an infinite bulk crystal into two semi-infinite parts, and so it is equal to the energy to be applied for the creation of two surfaces. In the supercell approach, E_{cleav} is calculated as the total energy difference per unit surface area. In slab calculations this value can be obtained as

$$E_{\text{cleav}} = (E_{\text{surf}} - E_{\text{bulk}}) / 2S, \tag{1}$$

where E_{surf} is the total energy of the supercell and E_{bulk} is the energy of the bulk unit cell containing the same number of atoms, *S* is the surface area. The number 2 in denominator accounts for the two surfaces within the slab supercell. If, in the above equation, E_{surf} is the energy of an unrelaxed slab, it will be denoted as $E_{\text{cleav}}^{\text{unrelaxed}}$, i.e., the cleavage energy of the

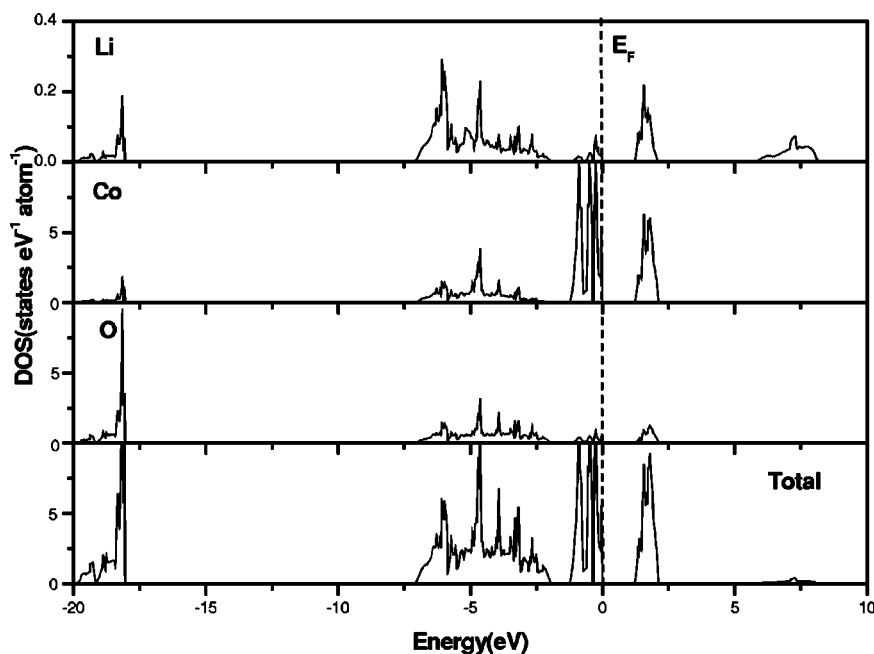


FIG. 4. DOS of bulk LiCoO₂ (bottom panel) together with local DOS on Co, O, and Li sites. In the case of total DOS one should read (formula unit)-1 instead of (atom)-1 in the density units description. The Fermi level is set to zero.

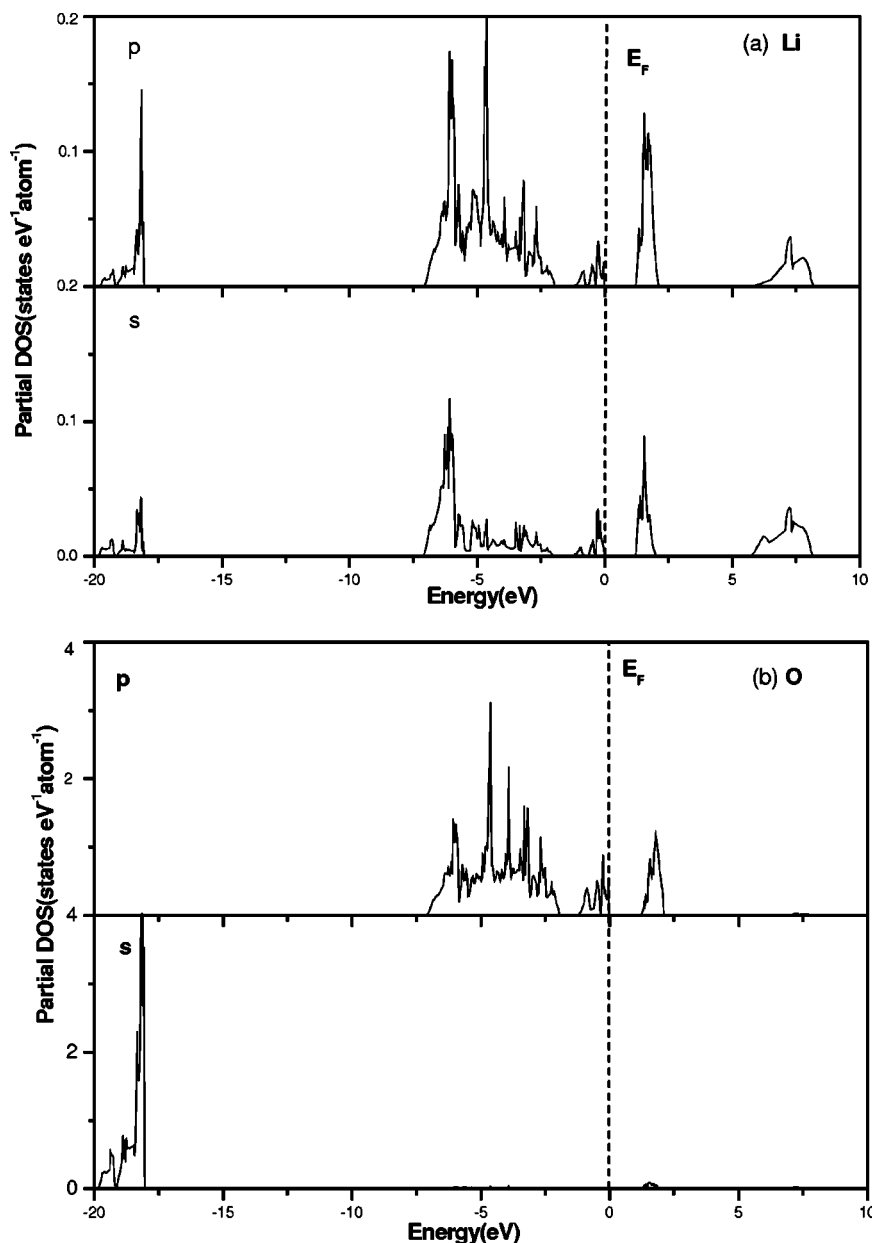


FIG. 5. Partial local DOS of (a) Li, (b) Co, and (c) O in LiCoO_2 . Fermi level is set to zero. When comparing contributions of states with different character note the different scale of some panels.

ideal, unrelaxed surface. When E_{surf} is the energy of the relaxed slab, we have the cleavage energy of relaxed slab ($E_{\text{cleav}}^{\text{relaxed}}$).

III. CLEAN (003) SURFACES

Since there is virtually no atomically resolved information about the structure and composition of crystalline LiCoO_2 surfaces available from experiment, we have to perform our theoretical investigation from a very basic point of view. In order to get a first ideal about the geometric and electronic properties of different LiCoO_2 polar surfaces, we focus here on a rather coarse comparison of subset of all possible (2×2) terminations of the low-index surfaces of trigonal LiCoO_2 .

A. The bulk structures

LiCoO_2 has the structure of $\alpha\text{-NaFeO}_2$, which belongs to the space group $R\bar{3}m$.²⁰ In Fig. 1, the unit cell, with param-

eters $a=5.6332 \text{ \AA}$, $\alpha=90^\circ$ and $c=14.08 \text{ \AA}$, $\gamma=120^\circ$ contains 12 chemical formula units, and the atoms occupy the following Wyckoff positions: Co: $3a(0,0,0)$, Li: $3b(0,0,0.5)$, O: $6c(0,0,x)$ with $x=0.260$. The prototype of this structure can be thought of as a fcc stacking of close packed oxygen layers with the metal ions residing in the octahedral sites.²¹ In LiCoO_2 , the Li and Co ions alternately reside in separate planes, leading to the fully layered structure of Fig. 1.

The first step was optimization of the bulk unit cell using the chosen basis set and computational parameters. The electronic wave functions were expanded in plane-wave basis set including planes up to a cutoff energy of 550 eV. For the bulk calculation, the supercell was built of 12 atomic layers containing 48 atoms and a $(4 \times 4 \times 2)$ Monkhorst-Pack¹⁸ k -point mesh was used. Again, a denser $(6 \times 6 \times 3)$ mesh did not alter the results. All atoms were fully relaxed by minimizing the forces acting on atoms.

TABLE II. Summary of the surface relaxations for *A*-type-O and -Li surfaces and *B*-type-O and -Co surfaces (see Fig 2). O and Li refer to the O- and Li-termination surfaces, respectively. Relative deviation from theory values of unrelaxed surface are given in parentheses.

Distance (Å)	Full relaxation			
	A-type-O	A-type-Li	B-type-Co	B-type-O
d_{12}	0.8808	0.9237	0.8094	0.9563
d_{23}	1.0789	1.1540	1.4685	1.7547
d_{34}	1.2480	0.9984	1.2415	0.9519
d_{45}	1.4418	1.4499	1.0590	1.0656
d_{56}	1.0037	1.2750	1.0107	1.2272
d_{67}	1.0489		1.4134	
Δd_{12}	-0.1591(-16%)	-0.3998(-30%)	-0.2305(-23%)	-0.3672(-28%)
Δd_{23}	+0.0390(+3.8%)	+0.1131(+11%)	+0.1450(+11%)	+0.4312(+33%)
Δd_{34}	-0.07550(-5.7%)	-0.0415(-4.0%)	-0.0820(-0.2%)	-0.0879(-8.5%)
Δd_{45}	+0.1183(+9.0%)	+0.1264(+9.5%)	+0.0191(+1.9%)	0.0257(+2.5%)
Δd_{56}	-0.0362(-3.5%)	-0.0549(-4.2%)	-0.0292(-2.9%)	-0.0963(-7.3%)
Δd_{67}	+0.0090(+0.87%)		+0.0899(6.8%)	

Within our PAW-GGA approach the optimized lattice constants of LiCoO_2 unit cell are obtained as $a=2.84 \text{ \AA}$, $c=14.18 \text{ \AA}$, which is in line with the experimental lattice parameter values ($a_{\text{exp}}=2.82 \text{ \AA}$, $c_{\text{exp}}=14.08 \text{ \AA}$).²² The computed and experiment values of the structural parameter for bulk LiCoO_2 are shown in Table I. The c/a ratio is almost identical to the experimental value in our calculations. The structure relaxation keeps the octahedron perfect, reducing the size of all the nearest-neighbor distances between oxygen layer and cobalt layer while increasing those distances between oxygen layer and lithium layer.

The amount of oxygen states mixed into Co d states (or vice versa) can be assessed from Fig. 4, which summarizes the contributions of Li, Co, and O to the total DOS. One may notice that d states of Co and p states of O dominate over all the other contributions to the valence bands (apart from the narrow band of oxygen $2s$ states at -19 eV). A much more detailed analysis can be made, however, on the basis of Figs. 5(a)–5(c) where local partial DOS's of Li, Co, and O, respectively, are given in the separate panels. The lowest band in the valence region is derived from the O ($2s$) states and centered at 19 eV or so below the Fermi level. This band has a weak dispersion, with a bandwidth around $1\text{--}2.5 \text{ eV}$, indicating the O ($2s$) electrons are localized. The valence band is mainly derived from the O ($2p$) and Co ($3d$) states which show a large dispersion than the O ($2s$) and Co ($4s$) bands, respectively, indicating significant delocalization (bandwidth about 6 eV). The conduction bands are derived mainly from the empty Co ($3d$) and from O ($2p$) valence states (around $\text{Co}:\text{O}=6$). The unoccupied states between 5.5 and 8 eV are dominated by Li s and p contributions.

Generally, the calculated eigenvalue band gaps are smaller than the corresponding experimental optical band gaps for the GGA and LDA. For LiCoO_2 , the calculated (direct) band gap is 1.77 eV , to be compared with the experimental optical band gap around 2.7 eV .²³

B. Cleavage energies

When a stoichiometric LiCoO_2 slab is ideally cut and the two parts are put apart, two complementary surface terminations are created. In our case, they are the *A*-type-O and *A*-type-Li terminations, on one hand, and the *B*-type-O and *B*-type-Co ones, on the other. The surfaces with both terminations arise simultaneously under cleavage of the crystal and relevant cleavage energy is divided between these two surfaces.

The (003) plane consists of only one type of atom (Co, O or Li), and so this plane is polar and causes some difficulties in the surface energy estimation. For nonpolar slabs, the surface energy is simply half of the cleavage energy, since the slab has two identical surfaces. For polar slabs, there are two different surface terminations in a slab calculation, and here no unique surface energy can be defined, and only the cleav-

TABLE III. Surface preliminary relaxation for *A*-type termination. Relative deviation from theory values of unrelaxed surface are given in parentheses.

Distance (Å)	Preliminary relaxation	
	A-type-O	A-type-Li
d_{12}	0.8800	0.9251
d_{23}	1.0753	1.1546
d_{34}	1.2786	1.0069
d_{45}	1.4059	1.4275
d_{56}	1.0101	1.2882
Δd_{12}	-0.1599(-16%)	-0.3984(-30%)
Δd_{23}	+0.0354(+3.4%)	+0.1147(+11%)
Δd_{34}	-0.0449(-3.4%)	-0.0330(-3.2%)
Δd_{45}	+0.0824(+6.2%)	+0.1040(+7.9%)
Δd_{56}	-0.0298(-2.9%)	-0.0353(-2.7%)

age energy of the crystal is well defined. To be able to compare the relative stability of the polar and nonpolar surfaces, as will be discussed, only the cleavage energies will be discussed in the following.

The calculated cleavage energies for the unrelaxed and relaxed (003) surfaces are given in Table IV. Our GGA results are presented for the 12-layer atoms for *A* and *B* types and the 13-layer atoms for nonpolar slab, as will be discussed in Sec. IV. The unrelaxed and relaxed cleavage energies for *A* type are 1.49 and 1.18 J/m² and for *B* type they are 3.81 and 3.47 J/m², respectively. Due to the obvious different cleavage energies, *A*-type surfaces can be formed more possibly than *B*-type ones. That is to say, the interactions between cobalt layer and oxygen layer are much stronger than those between lithium layer and oxygen layer, which agrees with results in Ref. 24. On the other hand, this conclusion can indirectly explain the phenomenon that LiCoO₂ coated by MgO possesses the more stable structure²⁵ because the exposed Li-O groups easily react with the electrolytes so that the structure is destroyed.

We have also calculated the energy gained by relaxation of ideally cut surface, the relaxation energy, calculated as $E_{\text{relaxed}} = -(E_{\text{surf}}^{\text{relaxed}} - E_{\text{surf}}^{\text{unrelaxed}})$. The relaxation energies are 0.028 eV per formula and 0.026 eV per formula for *A* type and *B* type, respectively. Although the different terminations of the (003) surface lead to great differences in the cleavage energy, the relaxation energies have almost no difference.

C. Surface geometry structure

There are several ways to minimize the energy of a cleaved surface, such as relaxation, surface reconstruction, and adsorption of adatoms on the surface. Here we have studied the relaxation of the surface atoms to their equilibrium positions. The energy gained was described above; here we will discuss the surface geometry structure.

For the LiCoO₂ (003) surfaces there are two different (2×2) surface terminations, one containing only O atoms in the topmost layer (*A*-type-O), and the other Li (*A*-type-Li),

as shown in Fig. 2(a). The other LiCoO₂(003) surfaces are also parallel to the *xy* plane, and there are again two (2×2) surface terminations, one with only O atoms (*B*-type-O) and one with Co ones (*B*-type-Co) in the topmost layer, as shown in Fig. 2(b). These four different (2×2) terminations are nonstoichiometric, exhibiting an excess of oxygen or cobalt/lithium atoms, and belong to the class of so-called polar surfaces,^{3,8} the stability issue of which will be discussed in Sec. IV.

As far as the atomic structure is concerned, important modifications are present on the surface. The relaxations of the metal and oxygen terminated surfaces are very large. Preliminary optimization of *A* type allowed motion in only the first five layers of atoms. For both types, the outermost layer atoms move inwards the surface, only in the direction perpendicular to the surface, to further decrease the thickness of the whole equilibrium atom layers. All atoms almost have no relaxation along the *xy* plane. Therefore, fully relaxation of these surface structures gives rise to a similar result in spite of a little difference. The extrapolated results for the preliminary and full relaxations of the polar surfaces are summarized in Tables II and III for *A* type and *B* type, respectively. For preliminary and full relaxations optimization, the largest relaxation is found for the *A* type Li termination, where the outermost interlayer spacing is compressed by about 30% relative to the bulk interlayer spacing, while the first double-layer distance of *A*-type O termination decreases by about 16%.

The outermost lithium and oxygen atoms of the *A* type surface shorten the thickness of whole equilibrium atom layers by about 0.25 and 0.12 Å, respectively. The second-layer Co atoms move by 0.04 Å in the direction opposite to that for the top-layer O atoms, whereas the third-layer O atoms displace by 0.003 Å outward, that is, in the same direction as the second-layer Co atoms. So the first and second interlayer spacing have relaxations of increase and decrease, respectively. From the top layer O to the bottom layer Li, the relaxations of all interlayer spacing decrease and increase alternately.

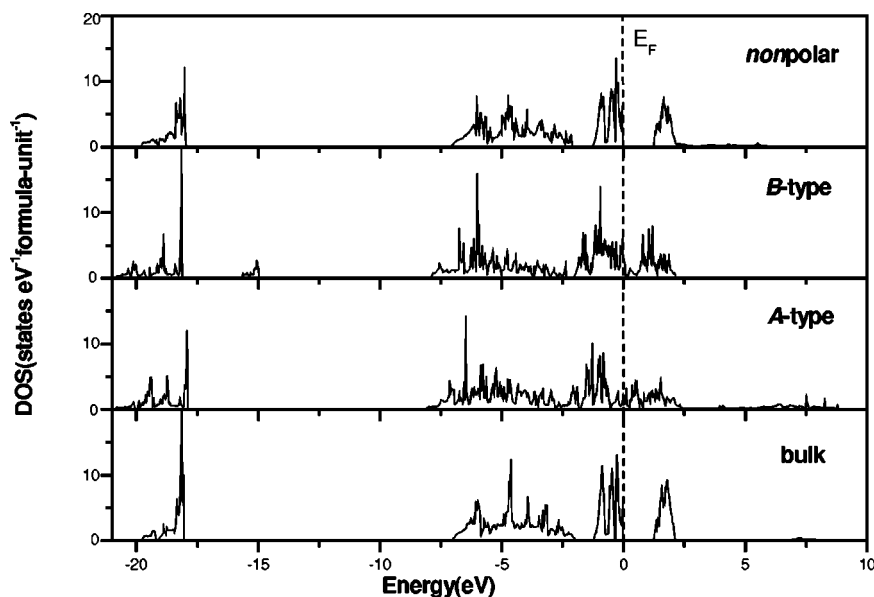


FIG. 6. DOS of bulk and both clean, and unreconstructed (003) surfaces of LiCoO₂. (a) the DOS of *A*-type termination, (b) the density of states of *B*-type termination, and (c) the density of states of both Li terminations. Fermi level is set to zero.

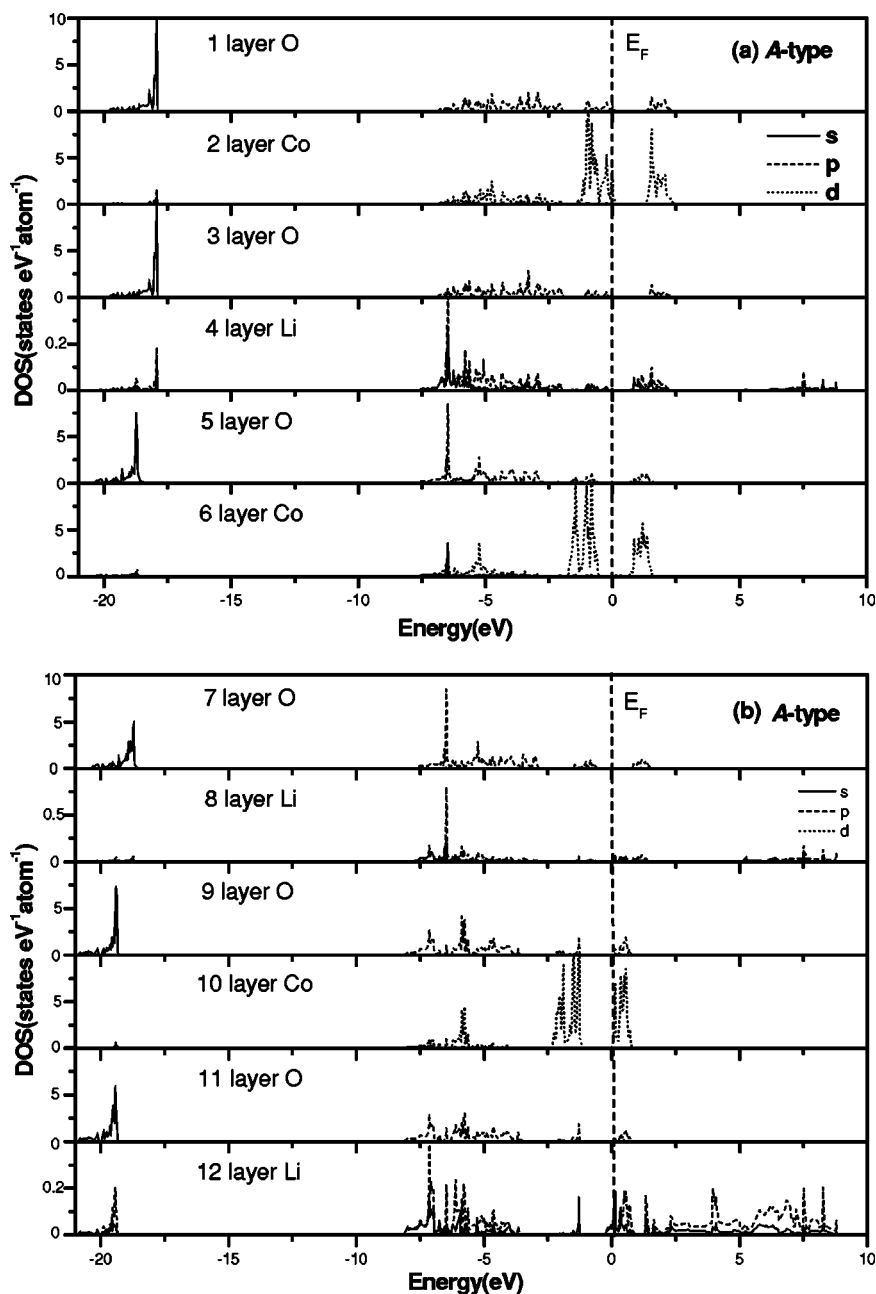


FIG. 7. Partial DOS of each atom from top layer to bottom layer for *A* and *B* types. *s*, *p*, and *d* states are presented with straight, dashed, and dotted lines, respectively. Fermi level is set to zero. When comparing contributions of states different character note the different scale of some panels.

For full relaxation, the outermost cobalt and oxygen atoms of the *B*-type surface sink into the thickness of atom-layer by about 0.12 and 0.38 Å, respectively. The largest relaxation is found for the *B*-type O-terminated surface, where the outermost interlayer spacing is lessened by roughly 27%, compared to the bulk value. However, the first double-layer distance of *B*-type Co termination is reduced by about 22%. The second-layer O atoms move by 0.13 Å outward, whereas the third-layer Li atoms move inward, by 0.11 Å. From the top layer O to the bottom layer Co, the changes of all interlayer spacing are alternative. More details are shown in Tables II and III. It is noticeable that the second interlayer spacing is lengthened, by 33%, in *B*-type O termination with respect to bulk value.

To summarize, both types of surfaces show the same basic relaxations with the outermost cation and anion moving in-

wards, resulting in a decrease of the thickness of the whole atom layer, independent on the terminations. The decrease and increase of relaxations of all interlayer spacing are alternative.

D. Surface electronic structures

The projected density of states (PDOS) for the atoms on the relaxed (003) surfaces were calculated and shown in Figs. 6 and 7. The corresponding DOS plots for bulk LiCoO₂ are also shown. The highest occupied band is mostly determined by the 3*d* states of cobalt, with some contributions from oxygen 2*p*, whereas the characteristic narrow peak above the Fermi level mainly consists of the 3*d* states of Co. The lowest energy band consists of oxygen 2*s* contributions. As with the case of bulk, the contributions of Li to DOS are

TABLE IV. Cleavage energy E_{cleav} (in J/m^2) and relaxation energy E_{relax} (in eV per chemical formula of LiCoO_2) for the different LiCoO_2 surfaces. The total energy is the energy calculated before the relaxation.

(003) surface	Total energy	$E_{\text{cleav}}^{\text{unrelaxed}}$	$E_{\text{cleav}}^{\text{relaxed}}$	E_{relax}
A type	-290.0738	1.49	1.18	0.31
B type	-277.0604	3.81	3.47	0.34
nonpolar	-293.2491	0.92	0.59	0.33

very small but not equal to zero. The surface bands are intersected by the Fermi level, which confers a metallic character to both *A*-type and *B*-type terminations.

The DOS of bulk LiCoO_2 calculated here with the PAW-GGA method is found to be very similar to the DOS curves resulting from the LSDA calculations in Ref. 24 and to the FLAPW calculations of bulk LiCoO_2 in Ref. 26. The DOS structures for the (003) surfaces show some resemblances to the DOS for the bulk, although some differences can be found (Figs. 5 and 6). For the surfaces some bands are shifted and the gaps reduced, compared to those in the bulk. In particular, there is no energy gap between the valence and conduction bands for the (003) surfaces due to the contributions of 10th layer cobalt $3d$ and outermost Li $1s/2p$ states and 11th layer Li and outermost O $2p$ states for *A* type and *B* type, respectively. Likewise, the lowest-energy band up shifts with respect to the Fermi level for the (003) surfaces. All bandwidths are expended lightly relative to the bulk, which are mainly resulted from O- $2p$ electronic redistribution, regardless of *A* or *B* type. For *B* type, furthermore, $2p$ states of the 12th layer O are localized in Fermi level, while the states of other O layers in *A* and *B* types are similar each other and show resemblances to those of the bulk.

Around the Fermi level, ranging from about -1.934 to 1.179 eV, the numbers of states are 5.727, 5.777, 6.886, and 10.716 (states unit^{-1}) for the bulk, nonpolar, *A* type and *B* type, respectively (see Fig. 6). Similarly, the corresponding energies of systems are also increasing (see Table IV). That is to say, the higher the system energy is, the bigger the number of DOS around Fermi level is, and the more obvious the changes of DOS are. For *A* type the redistribution of Co- $3d$ and for *B* type the redistribution of Co- $3d$ and O- $2p$ have the main responsibility for the changes of states closing to Fermi level, respectively (see Fig. 7). Also the changes occur at the cost of the state number of conduct band relative to the bulk. Furthermore, we can also see that the polarity has an important influence on the electronic redistribution (see Fig. 6). *A* type and *B* type are polar, and they show metallic characters; but the case is not true for nonpolar surface, and the number of states from about -1.934 – 1.179 eV has no obvious difference between the nonpolar surface and the bulk.

All in all, it is clear that the introduction of a surface in stoichiometric LiCoO_2 affects the electronic structure in the surface layers to some extent. Furthermore, *A* type and *B* type have the metallic character due to the introductions of surfaces.

TABLE V. Relaxation and rumpling on the (003)- LiCoO_2 terminations. The mean positions of the LiCoO_2 layers are computed by averaging the normal coordinates of the corresponding atoms. The interplanar distances are given in angstroms and their relative variations in brackets. The displacements of the i th (d_1, d_2) layer surface atoms, and the rumpling amplitudes $r \equiv d_1 - d_2$ are given in Å. “+” and “-” mean increase and decrease, respectively.

Layer	Relaxations (Å)		Rumpling (Å)
	d_1	d_2	$d_1 - d_2$
1 Li	-0.3994		no rumpling
↑	0.9085(-32%)		
2O	0.0430	-0.0118	0.0548
↑	1.0199(-1.9%)		
3Co	0.0475	0.0237	0.0238
↑	1.0273(-1.2%)		
4O	0.0579	0.0385	0.0293
↑	1.3501(+2.0%)		
5Li	0.0257	0.0166	0.0091
↑	1.3575(+2.6%)		
6O	-0.0127	-0.0120	-0.0007
↑	1.0275(-1.2%)		
7Co	0.0003	-0.0003	0.0006

IV. NONPOLARIZED (003) SURFACES

As mentioned above, all of the four possible (2×2) terminations are nonstoichiometric and are called as polar surfaces, which are usually not expected to be stable on electrostatic grounds.⁴ Various mechanisms can also be imagined for the stabilization of polar surfaces of LiCoO_2 (003). For this system, the polar (003) surface was modeled as a Li-terminated surface with half of the surface Li atoms moved from one side of the slab to the other in one checkerboard way to eliminate the dipolar moment and to fill the LiCoO_2 formula. The lithium termination considered here is schematically shown in Fig. 3: the lithium atoms are located along [003] on both surfaces of the slab as in Fig. 4(a).

As far as the atomic structure is concerned, it can be seen in Table V that large relaxations occur in the outermost layers. The interlayer distance between the outermost Li layer without rumpling and the next layer O with neglectable rumpling beneath the outermost Li layer contracts by 32%, while that between the latter and the third Co layer is compressed by 1.9%. The largest relaxation is equal to 0.40 Å and inwards in the outermost Li layers, while the rumpling of other layers has no much influence. Due to the relaxations of outermost Li layers, the thickness of the atom layer is decreased by 0.80 Å relative to the bulk value. Fortunately, the distances of Li-O interlayer and that of Co-O interlayer are increased and decreased, respectively, except for the contraction of the outermost Li-O interlayer distance, which would be helpful to the motion of Li ions during the intercalation/deintercalation process in Li-ion batteries.

Unlike *A* or *B* type, the DOS plots of the nonpolar surfaces are almost identical with those of the bulk, except for

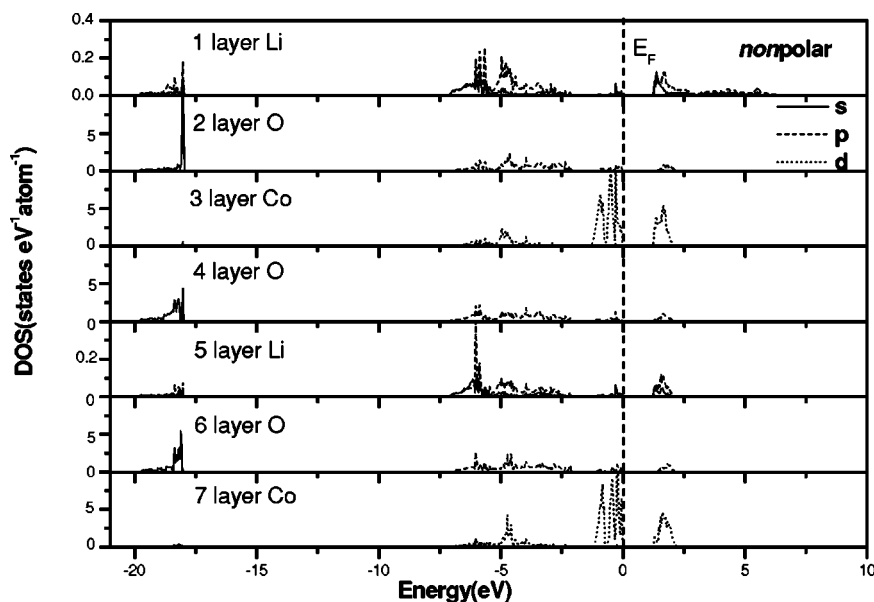


FIG. 8. Similar to Fig. 7 but for nonpolar surfaces.

the neglectable difference between the outermost Li of the nonpolar surfaces and the Li of the bulk (see Figs. 6 and 8). The surface bands are kept a semiconductor character rather than a metal character due to the symmetry of the nonpolarized surface.

From the energy point of view, more importantly, the cleavage energies of unrelaxed and relaxed nonpolar surfaces, which are 0.92 and 0.59 J/m², respectively (see Table IV), are much smaller than those of *A* type (not mention to *B* type). Obviously, the nonpolar surfaces are more stable than the clean and unreconstructed polar surfaces, indicating the possibility of the reconstruction of the polar (003) surfaces.

Unfortunately, to our knowledge, no experimental information on such surface reconstructions is presently available for crystalline LiCoO₂. Without any such information, not even on the surface periodicity, the phase space of possible reconstructions is simply too huge to be assertively screened by today's first-principles techniques alone.²⁷ Compared to the construction presented in this study, the best we can do is to check by how much surface reconstructions would have to lower the surface free energy, when such information becomes available from experiments, in order to give rise to significant changes in the real LiCoO₂ crystal shape.

V. CONCLUSION

We have performed a theoretical study of the atomic structures, electronic structures, and the cleavage energies of the (003) polar surfaces of stoichiometric LiCoO₂, through a first-principles pseudopotential approach that has been carried out within the density-functional theory. Our calculations show that the clean, unreconstructed relaxed (003) surface displays differences compared to the DOS for bulk LiCoO₂, while the DOS of the nonpolar surface is very bulk-

like. For the surfaces some bands of *A* and *B* type are shifted and the gaps are reduced and show a metallic character, while the semiconductor character is retained in the nonpolar surface considered in this study. For all surfaces we obtain a considerable inwards relaxation of the surface atoms and a strong contraction of the outermost double-layer spacing. For the nonpolar surface model, the relaxations are beneficial to the motion of lithium ions in the charge and discharge process. On the other hand, because the exposed Li-O groups easily react with the electrolytes so that the structure is destroyed, this can indirectly explains the phenomenon that LiCoO₂ coated by MgO possesses the more stable structure. As far as the unreconstructed ideal surfaces, the surfaces are formed much easier by breaking the Li-O interaction than by breaking the Co-O interaction along the direction perpendicular to the *c* axis. However, the nonpolar surfaces occupy lower cleavage energy, implying the possibility of the reconstruction of (003) surfaces.

Although there is no experimental evidence concerning whether the unreconstructed or reconstructed surfaces, the main results of the presented investigation are an available set of reliable data for the LiCoO₂ (003) surfaces, which we consider to be a reference for future studies.

ACKNOWLEDGMENTS

We acknowledge the financial support from Youth Scientific Project of Jiangxi Normal University (Grant No. 1075), Open Project of Key Laboratory for Opt-electronics of Jiangxi Province (Grant No. 2004003), National Science Foundation of China (NSFC) (Grant No. 59972041), National 973 key program of China (Grant No. 2002CB211802) and Science Foundation of JiangXi Province (Grant No. 0321019).

*Electronic address: jxsdjyh@yahoo.com.cn

†Electronic address: lqchen@aphy.iphy.ac.cn

- ¹*Lithium Batteries*, edited by G. Pistoia (Elsevier, Amsterdam, 1994).
- ²R. B. Goldner, R. L. Chapman, G. Foley, E. L. Goldner, T. Haas, P. Norton, G. Seward, and K. K. Wong, *Sol. Energy Mater.* **14**, 195 (1986).
- ³C. Noguera, *J. Phys.: Condens. Matter* **12**, R367 (2000).
- ⁴P. W. Tasker, *J. Phys. C* **12**, 4977 (1979).
- ⁵C. Noguera, *J. Phys.: Condens. Matter* **12**, R367 (2000).
- ⁶C. Noguera, A. Pojani, P. Casek, and F. Finocchi, *Surf. Sci.* **507-510**, 245 (2002).
- ⁷P. E. Blöchl, *Phys. Rev. B* **50**, 17 953 (1994).
- ⁸P. Hohenberg and W. Kohn, *Phys. Rev.* **136**, B864 (1964); W. Kohn and L. Sham, *Phys. Rev.* **140**, A1133 (1965).
- ⁹J. P. Perdew, J. A. Chevary, S. H. Vosko, K. A. Jackson, M. R. Pederson, D. J. Singh, and C. Fiolhais, *Phys. Rev. B* **46**, 6671 (1992).
- ¹⁰J. P. Perdew and Y. Wang, *Phys. Rev. B* **45**, 13 244 (1992).
- ¹¹N. A. W. Holzwarth, G. E. Matthews, R. B. Dunning, A. R. Tackett, and Y. Zeng, *Phys. Rev. B* **55**, 2005 (1997).
- ¹²G. Kresse and D. Joubert, *Phys. Rev. B* **59**, 1758 (1999).
- ¹³G. Kresse and J. Hafner, *Phys. Rev. B* **47**, 558 (1993); **49**, 14 251 (1994).
- ¹⁴G. Kresse and J. Furthmüller, *Comput. Mater. Sci.* **6**, 15 (1996); *Phys. Rev. B* **54**, 11 169 (1996).
- ¹⁵G. Ceder, M. K. Aydinol, and A. F. Kohan, *Comput. Mater. Sci.* **8**, 161 (1997).
- ¹⁶T. Ohzuhu, A. Ueda, Y. Iwakoshi, and H. Komori, *Electrochim. Acta* **38**, 1159 (1993).
- ¹⁷M. K. Aydinol, A. F. Kohan, and G. Ceder, *Phys. Rev. B* **56**, 1354 (1997).
- ¹⁸H. J. Monkhorst and J. D. Pack, *Phys. Rev. B* **13**, 5188 (1976).
- ¹⁹C. -L. Fu and K. M. Ho, *Phys. Rev. B* **28**, 5480 (1983).
- ²⁰A. Van der, M. K. Aydinol, and G. Ceder, *Phys. Rev. B* **58**, 2975 (1998).
- ²¹H. J. Orman and P. J. Wiseman, *Acta Crystallogr., Sect. C: Cryst. Struct. Commun.* **40**, 12 (1984).
- ²²J. N. Reimers and J. R. Dahn, *J. Electrochem. Soc.* **139**, 2091 (1992).
- ²³J. van Elp, J. L. Wieland, H. Eskes, P. Kuiper, G. A. Sawatzky, F. M. de Groot, and T. S. Turner, *Phys. Rev. B* **44**, 6090 (1991).
- ²⁴M. T. Czyzyk, R. Potze, and G. A. Sawatzky, *Phys. Rev. B* **46**, 3729 (1992).
- ²⁵Zhaoxiang Wang, Chuan Wu, Lijun Liu, Feng Li, Liquan Chen, J. Electrochem. Soc. **149**, A466 (2002).
- ²⁶M. K. Aydinol, A. F. Kohan, and G. Ceder, *Phys. Rev. B* **56**, 1354 (1997).
- ²⁷E. Lundgren, G. Kresse, C. Klein, M. Borg, J. N. Andersen, M. De Stantis, Y. Gauthier, C. Konvicka, M. Schmid, and P. Varga, *Phys. Rev. Lett.* **88**, 246103 (2002).